

# Wildfires in the Larch Range within Permafrost, Siberia

Viacheslav I. Kharuk <sup>1,2,3,\*</sup> , Evgeny G. Shvetsov <sup>2</sup>, Ludmila V. Buryak <sup>2</sup>, Alexei S. Golyukov <sup>1,2,3</sup> ,  
Maria L. Dvinskaya <sup>2,3</sup>  and Il'ya A. Petrov <sup>1,2,3</sup> 

<sup>1</sup> School of Space and Information Technologies, Siberian Federal University, Svobodny Str. 79, 660041 Krasnoyarsk, Russia; golyukov@ksc.krasn.ru (A.S.G.); petrov.ia@ksc.krasn.ru (I.A.P.)

<sup>2</sup> Sukachev Institute of Forests, Federal Scientific Center, Russian Academy of Science, Siberian Branch, Akademgorodok 50/28, 660036 Krasnoyarsk, Russia; inter@ksc.krasn.ru (E.G.S.); buryaklv@firescience.ru (L.V.B.); mary\_dvi@ksc.krasn.ru (M.L.D.)

<sup>3</sup> Laboratory of Biodiversity and Ecology, Tomsk State University, Lenin Str. 36, 634050 Tomsk, Russia

\* Correspondence: v7sib@mail.ru

**Abstract:** Throughout the larch range, warming leads to frequent fires and an increase in burned areas. We test the hypothesis that fires are an essential natural factor that reset larch regeneration and support the existence of larch forests. The study area included *Larix sibirica* and *L. gmelinii* ranges within the permafrost zone. We used satellite-derived and field data, dendrochronology, and climate variables analysis. We found that warming led to an increase in fire frequency and intensity, mean, and extreme (>10,000 ha) burned areas. The burned area is increasing in the northward direction, while fire frequency is decreasing. The fire rate exponentially increases with decreasing soil moisture and increasing air temperature and air drought. We found a contrasting effect of wildfire on regeneration within continuous permafrost and within the southern lowland boundary of the larch range. In the first case, burnt areas regenerated via abounded larch seedlings (up to 500,000+ per ha), whereas the south burns regenerated mostly via broadleaf species or turned into grass communities. After the fire, vegetation GPP was restored to pre-fire levels within 3–15 years, which may indicate that larch forests continue to serve as carbon stock. At the southern edge of the larch range, an amplified fire rate led to the transformation of larch forests into grass and shrub communities. We suggested that the thawing of continuous permafrost would lead to shrinking larch-dominance in the south. Data obtained indicated that recurrent fires are a prerequisite for larch forests' successful regeneration and resilience within continuous permafrost. It is therefore not necessary to suppress all fires within the zone of larch dominance. Instead, we must focus fire suppression on areas of high natural, social, and economic importance, permitting fires to burn in vast, larch-dominant permafrost landscapes.

**Keywords:** wildfires in permafrost; larch; forest fires; extreme fires; climate-driven fires; firefighting; fire



**Citation:** Kharuk, V.I.; Shvetsov, E.G.; Buryak, L.V.; Golyukov, A.S.; Dvinskaya, M.L.; Petrov, I.A. Wildfires in the Larch Range within Permafrost, Siberia. *Fire* **2023**, *6*, 301. <https://doi.org/10.3390/fire6080301>

Academic Editor: Adrián Regos

Received: 20 June 2023

Revised: 27 July 2023

Accepted: 30 July 2023

Published: 4 August 2023



**Copyright:** © 2023 by the authors. Licensee MDPI, Basel, Switzerland. This article is an open access article distributed under the terms and conditions of the Creative Commons Attribution (CC BY) license (<https://creativecommons.org/licenses/by/4.0/>).

## 1. Introduction

Wildfires are a powerful ecological and evolutionary factor that force species traits and interactions, forest composition, nutrient cycling, and ecosystem function [1–4]. In recent decades, boreal forests, including Siberian taiga, have experienced an increasing influence of fire frequency [5–9]. In extreme years, the fire-affected areas in Siberia have exceeded 12 MH [9].

In the boreal region, a major factor of fire rate amplification is warming, which has driven increases in lightning frequency and fuel flammability [10,11]. Although globally warming will decrease the frequency of lightning strikes, it is projected that at high latitudes, lightning strikes will continue to increase [12]. Fire rate amplification has even been observed in the Siberian Arctic, where the fire occurrence boundary is migrating northward and has already reached the Arctic Ocean coast in eastern Siberia [13]. In the face of the increasing severity of fire regimes, ecologists have determined that we need to learn how to

co-exist with the amplifying fire rate [1,2,4–6,9,13–15]. Research is increasingly focusing on firefighting strategy adaptation, as well as studying the ecological role of fires in supporting forest health and biodiversity [13,16,17]. It is known that the complete suppression of forest fires leads to fuel accumulation which, in some forests stands, that can result in catastrophic fires. At a landscape level, natural fires may be considered as a tool in mega fire suppression, as other methods are not applicable across extensive boreal ecosystems [17–19].

The growing knowledge of the ecological importance of wildfire, especially for pyrophytic species such as larch, is being increasingly acknowledged [4,13,20]. Thus, in the North American forests formed by *Larix laricina*, a greater dynamism was found in the wildfire-affected sites compared to the fire-excluded ones. At the wildfire site, tree populations are turning over faster, regenerating trees are growing faster, and more wood debris is available for decomposition [21]. Similarly, fires increase European larch (*Larix decidua*) regeneration [22]. In northern Siberia, larch (*L. sibirica*, *L. gmelinii*) has successfully regenerated within burned areas. However, at the sites with long fire return intervals, regeneration is poor and is not sufficient for supporting larch dominance [9,23].

In Siberia, the majority of fires occurred in the permafrost zone of larch-dominance [4,10,11]. Forests formed by *Larix sibirica*, *L. gmelinii*, and *L. cajanderi* occupy a territory of about 310 MH in the permafrost zone. This is the largest forest community in Siberia (i.e., approximately 60% of the forests). Larch is known as the most cold-resistant Siberian species and has thereby adapted to the severe permafrost climate. All larch species evolved under conditions of periodic fires, have adapted to the influence of fires, and have obtained advantages against non-fire-adapted species [9,21,22]. Recent studies have shown an increase in larch growth increment as a response to warming [24,25]. Meanwhile, an amplified fire rate within larch-dominant communities might be a challenge for the resilience of larch to the influence of wildfires.

Larch-dominant communities within permafrost are considered the largest pool of carbon in Eurasia. Presently, larch forests, as well as Russian forests as a whole, have served as a sink of carbon, although there is a danger of transforming them into a carbon source [26,27].

Given the amplified fire rate, it is required (i) to extend and deepen our knowledge on the fire rate and its relationship with environmental variables; (ii) to understand the influence of wildfires on the tree species resilience; and (iii) to improve/adapt the firefighting strategy. In this paper, we have analyzed the influence of wildfires on the larch (*Larix sibirica*, *L. gmelinii*) forests that are growing within the permafrost zone of Siberia. We hypothesized that (i) fires are a prerequisite natural factor that support successful larch regeneration, larch forest vigor, and larch dominance in the permafrost zone; and (ii) warming leads to an increase in burned areas, fire frequency, and intensity.

We seek answers to the following questions:

1. What are the temporal and spatial dynamics of the burned areas, fire numbers, and severity in the larch forests growing in the permafrost zone?
2. What is the influence of fires on larch growth and regeneration within permafrost?
3. What are the patterns of post-fire GPP recovery within burns?
4. What should be the approach to firefighting in the zone of larch dominance within permafrost?

## 2. Materials

### 2.1. Study Area

We have analyzed the fire rate in the larch forests formed by *Larix sibirica*, *L. gmelinii*, and *L. cajanderi* in the permafrost zone. Test sites were selected within larch-dominant stands located in continuous, discontinuous, sporadic, and patched permafrost. The southern part of the larch range is located in discontinuous, sporadic, and patched permafrost (Figure 1). We used the Arctic permafrost and ground ice map developed by the National Snow and Ice Data Center (NSIDC) and available online [28]. In continuous permafrost zone and the Trans-Baikal zone, forest are formed by *L. sibirica* and *L. gmelinii* (with some proportion of *Pinus sylvestris* L. in the Trans-Baikal zone) (areas #1 and #3 in

Figure 1). In the southern part of Altai–Sayan Mountains, *L. sibirica* is a dominant species (area #2 in Figure 1). The map of species composition within the study area is presented in Figure S1 [29]). We considered the dynamics of fire frequency and mean and total burned area for all and extreme (>10,000 ha) fires. We used on-ground survey and satellite data, dendrochronology-based tree growth, and climate variables analysis.

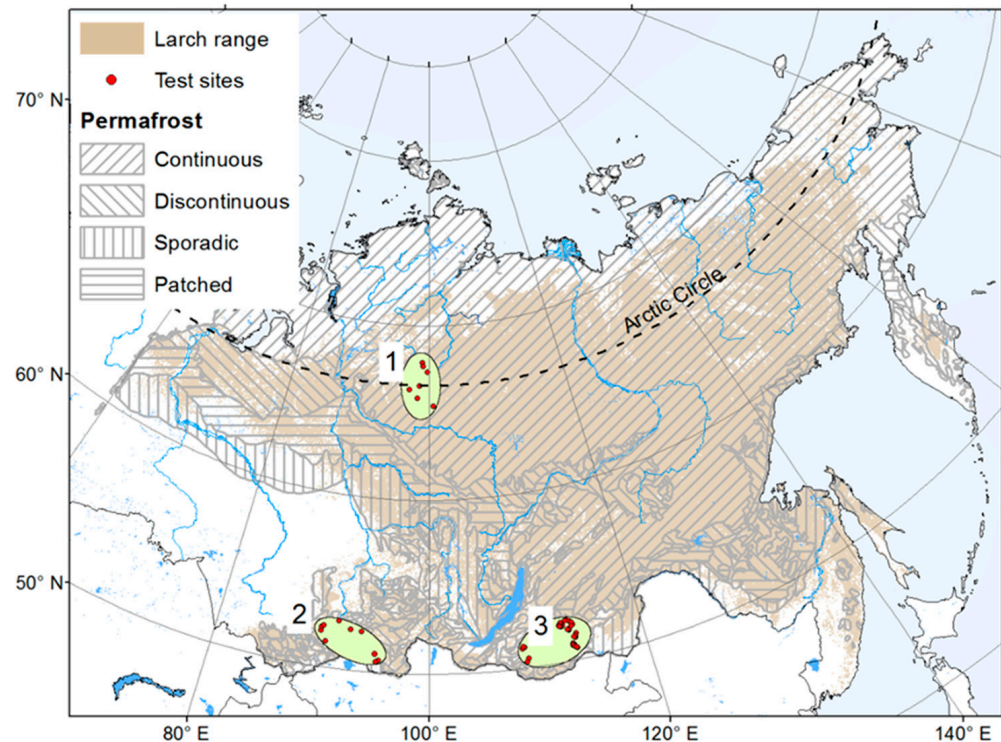


**Figure 1.** Larch range within permafrost area (marked by brown). Green ellipsoids indicate study areas located in continuous (site #1: “North”), and (sites #2: South1 in Altai–Sayan Mountains; and #3: South2 in the Trans–Baikal zone) in discontinuous, sporadic, and patched permafrost zones. Test sites’ (generalized) locations are marked by red dots. The test site’s number (N) is 28, 32, and 100 in the study area 1, 2, and 3, respectively.

## 2.2. Environmental Variables

Monthly air temperature, precipitation, and soil moisture content with a spatial resolution of  $0.1^\circ \times 0.1^\circ$  were obtained from the ERA5-Land dataset (2000–2022; <https://cds.climate.copernicus.eu/cdsapp#!/dataset/reanalysis-era5-land-monthly-means?tab=overview> (accessed on 9 June 2023) [30]. In the analysis, we used data for 0–7, 7–28, and 28–100 cm soil depth layers. Monthly values of the drought index SPEI (the Standardized Precipitation Evapotranspiration Index) were obtained from the Global Drought Monitor (<https://spei.csic.es/map/maps.html>; accessed on 9 June 2023) service for period 2000–2022. The SPEI is a measure of air moisture content (or air drought), and it is defined as the difference between total precipitation and potential evapotranspiration. Thus, by definition, the SPEI increase indicated an air drought decrease [31]. We also involved terrestrial water content (or EWTA, Equivalent of Water Thickness Anomalies—hereafter, TW) in the analysis. TW content is the product of gravimetric measurements (in  $\text{cm}^{-1}$ ) performed by the GRACE/GRACE-FO satellites with on-ground resolution  $1^\circ \times 1^\circ$  [32]. Monthly EWTA data were obtained from the GFZ database (<https://podaac-opendap.jpl.nasa.gov/opendap/hyrax/allData/tellus/L3> (accessed on 9 June 2023)) for period 2002–2022.

### 3. Methods

#### 3.1. Fire Rate Detection and Analysis

To map fire events, we used the geospatial fire database created in the Sukachev Institute of Forest, SB RAS. This database uses satellite fire detections obtained from the NOAA/AVHRR, TERRA/AQUA/MODIS, and SNPP/NOAA-20/VIIRS platforms. This database has been maintained since 1996. Fire radiative power (FRP) was estimated using MODIS thematic thermal anomaly product (MOD14/MYD14) [33]. The product contains data on coordinates, the detection time of a thermal anomaly, and FRP values with a spatial resolution of ~1000 m. Thermal anomaly products were downloaded using the LAADS (Level-1 Atmosphere Archive and Distribution System) service (<https://ladsweb.modaps.eosdis.nasa.gov>; accessed on 11 May 2023). We used settlement data from Open Street Map (<https://www.openstreetmap.org/>) to exclude thermal anomalies of anthropogenic origin, i.e., we excluded “fire” pixels located within settlement boundaries from further analysis. We also excluded thermal anomalies related to gas flares in oil and gas fields using high-resolution data from Google Earth. These gas flares were mainly located in the northwestern part of the study area.

#### 3.2. Regeneration Rate Analysis within Burns

We have studied the post-fire larch regeneration rate within burns located in the core part of the larch range (in continuous permafrost, study area #1 in Figure 1) and in the southern part of the larch range (areas #2 and #3), located in discontinuous, sporadic, and patched permafrost.

Our test sites (TS) have an area of 0.1 ha and a radius of 17.8 m [34]. We determined TS coordinates, terrain characteristics, soil type, time since the last fire, presence of dead wood, and amount of woody debris. All trees with a diameter at breast height (1.3 m) of 4 cm or greater were measured on each TS. The measurements included species composition, trees diameters, heights, presence of trunk, roots damage caused by fire, and (/or) other factors. We recorded seedlings in accordance with the regulations for reforestation manual [35], i.e., at least ten square (2 × 2 m or 1 × 1 m) plots were established within the test site. The seedlings were recorded considering five height groups: <0.10 m; 0.11–0.25 m; 0.26–0.50 m; 0.51–1.5 m; and >1.5 m. The seedlings were categorized as either healthy, weakened, or dead. Seedlings were considered healthy if over the last three years, the growth of the axial shoot exceeded the growth of neighboring lateral shoots, and it has green needles without mechanical, insect, and/or pathogen damage. Within each TS on-ground cover (grasses, moss, and lichen) species composition was described.

#### 3.3. Dendrochronology Analysis

To develop tree-ring chronologies, establish wildfire dating, and calculate fire-return intervals (FRI), we used 20 larch (*L. gmelinii*) samples (discs) with fire scars (coordinates of test sites' center point are 65°20'N/100°37'E). In addition, one unique sample of *L. sibirica* with 13 fire scars was used in the analysis (test site coordinates: 61°36' N, 93°00' E). The surface of each disk was sanded and treated with a contrasting powder. The tree ring widths were measured with an accuracy of 0.01 mm using the LINTAB-6 platform. We used master-chronology of northern larch trees from [36] for dating the fire scars and building the FRI chronology. That chronology was used to determine FRI by fire scars crossdating. Crossdating quality was estimated using the COFECHA and TSAP software [37]. The widths of tree rings in millimeters were converted into the unitless growth index (GI). To reduce the effect of long-term age trends, each tree ring series was fitted with a negative exponential or negative linear trendline in ARSTAN software [38]. For *L. gmelinii*, we built the standard chronology as the robust mean of indexed chronologies for each tree sample. For *L. sibirica*, we used only one tree sample to develop chronology. To construct the FRI chronology, the FHAES program [39] was used. The superposed epoch analysis (SEA [40]) was used to estimate deviations in radial increment in the post-fire period.

### 3.4. GPP (Gross Primary Productivity) Dynamics

To estimate post-fire vegetation recovery, we analyzed the temporal dynamics of the gross primary productivity (GPP) for the burned areas. Annual GPP values were obtained from the Terra/MODIS product MOD17A3HGF at temporal and spatial resolutions of 8 days and 500 m, respectively (<https://search.earthdata.nasa.gov> (accessed on 25 May 2023)) [41].

### 3.5. Statistics

To characterize the degree of fire disturbance, we used the relative burned area (RBA) and relative number of fires (RNF) metrics. Relative burned area (RBA) was calculated as follows:

$$\text{RBA} = 100\% \frac{S_{\text{burned}}}{S_{\text{larch}}}, \quad (1)$$

where  $S_{\text{burned}}$  is mean annual burned area (ha);  $S_{\text{larch}}$  is the area of larch forests (ha).

At the same time, relative number of fires (RNF) was calculated as the number of fires per 100 thousand ha of larch forests:

$$\text{RNF} = 10^5 \frac{N_f}{S_{\text{larch}}}, \quad (2)$$

where  $N_f$  is number of fire events;  $S_{\text{larch}}$  is the area of larch forests (ha).

To perform calculations, we used MS Excel and ArcGIS (with NumPy and SciPy python modules) software. We used Wilcoxon rank sum test to assess between-group differences in fire radiative power. For instance, we used this approach to calculate differences between the FRP values in southern and northern latitudinal belts of Siberia as discussed further below. For the regression analysis, we used Statsoft Statistica software (<https://www.statistica.com> (accessed on 9 June 2023)).

## 4. Results

### 4.1. Climate Variables Dynamics within the Study Area

Increasing trends in the air temperature were observed within all study areas, whereas precipitation were stagnated or decreasing (Figure 2(a<sub>1</sub>,a<sub>2</sub>,b<sub>1</sub>,b<sub>2</sub>)). Soil moisture content was decreased for all sites (with the exception of the last 3 years (Figure 2(c<sub>1</sub>,c<sub>2</sub>)). Similarly, SPEI and TW (terrestrial water content) values also decreased (with the exception of the southern areas in case of TW (Figure 2(d<sub>1</sub>,d<sub>2</sub>,e<sub>1</sub>,e<sub>2</sub>))). Note that the SPEI index decrease indicates an air drought increase by definition. Thus, within all study areas, an increasing aridity was observed.

### 4.2. Wildfire Geography

Relative number of fires (RNF, i.e., fires per 100,000 ha of forests) has the highest value in the middle of the central Siberia and in the southern part of the larch range (Trans-Baikal area, Figure 3a). As discussed further, that was related to the soil moisture content and air temperature (Figures S2–S4; Table 1).

Geographically, extreme large burns occurred mostly in the southern and northern parts of the larch range (Figures 3b and 4). It is known that in the southern part of the larch range, fires were mostly caused by humans; whereas in the northern part, fires were mostly caused by lightning [13].

Along the geographic latitude, the burned area and the number of fires are changing synchronously (Figure 4). Both variables reach maximum values within the southern and northern parts of the larch range, whereas minimum values are observed within mid-latitudes (55°–59°). The latter refers to forests fragmentation and better fire suppression in this territory. At the same time, mean burned area is increasing in the northward direction, having maximum values between 65° and 71°, which was attributed to the higher values of available “fuel”. Furthermore, wildfires are not actually suppressed in those remote areas.

A sharp decrease is observed at higher latitudes, referring to the lower insolation which led to insufficient fuel dryness.

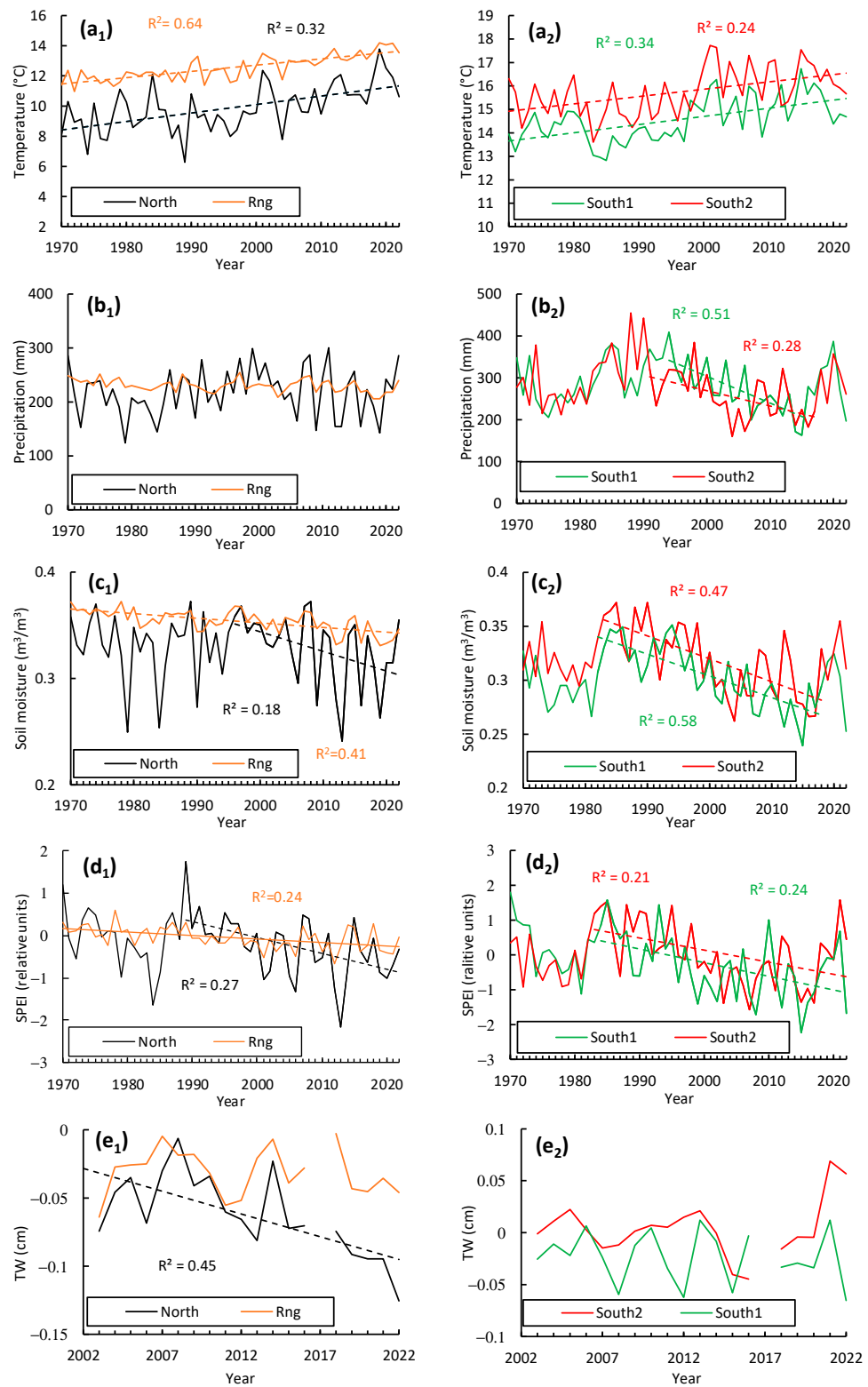


**Figure 2.** Temporal dynamics of summer (JJA) (a<sub>1</sub>,a<sub>2</sub>) air temperature, (b<sub>1</sub>,b<sub>2</sub>) precipitation, (c<sub>1</sub>,c<sub>2</sub>) soil moisture (0–7 cm), (d<sub>1</sub>,d<sub>2</sub>) SPEI drought index, and (e<sub>1</sub>,e<sub>2</sub>) terrestrial water content. Abbreviations: Rng—total larch range within the permafrost zone; North, South1, and South2—areas 1, 2, and 3 on Figure 1, respectively. All trends are significant at  $p < 0.05$ .

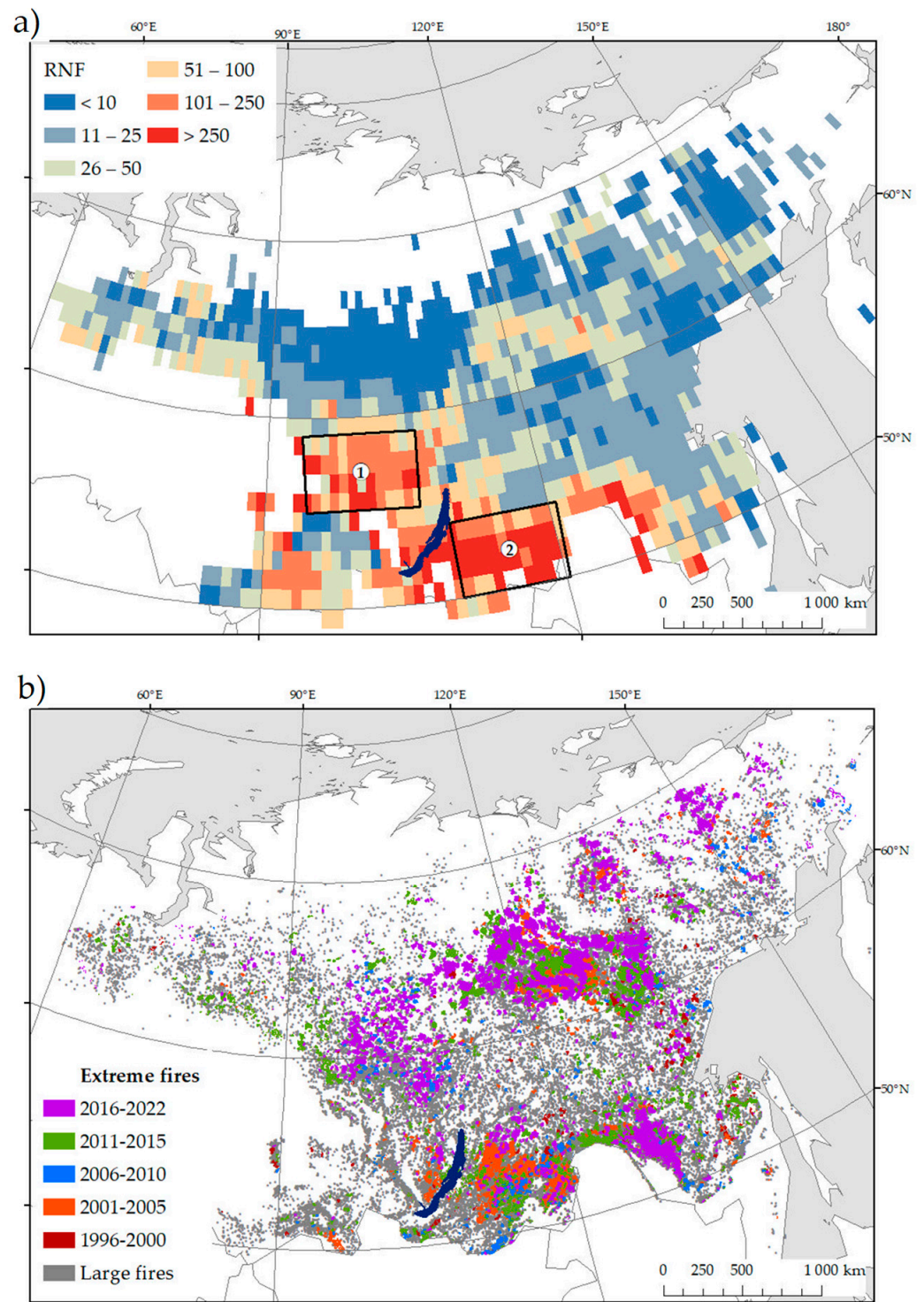


**Figure 3.** Maps of (a) relative number of fires (RNF) and (b) large ( $200 \text{ ha} < \text{burned area} \leq 10,000 \text{ ha}$ ) and extreme fires (burned area  $> 10,000 \text{ ha}$ ) within the larch range. Large fires are indicated by grey color. The largest number of fires was observed in (1) the middle of the Central Siberia; and (2) in the Trans-Baikal area. Extreme fires were mostly located in the southern and northern parts of the larch range. Study period is 1996–2022.

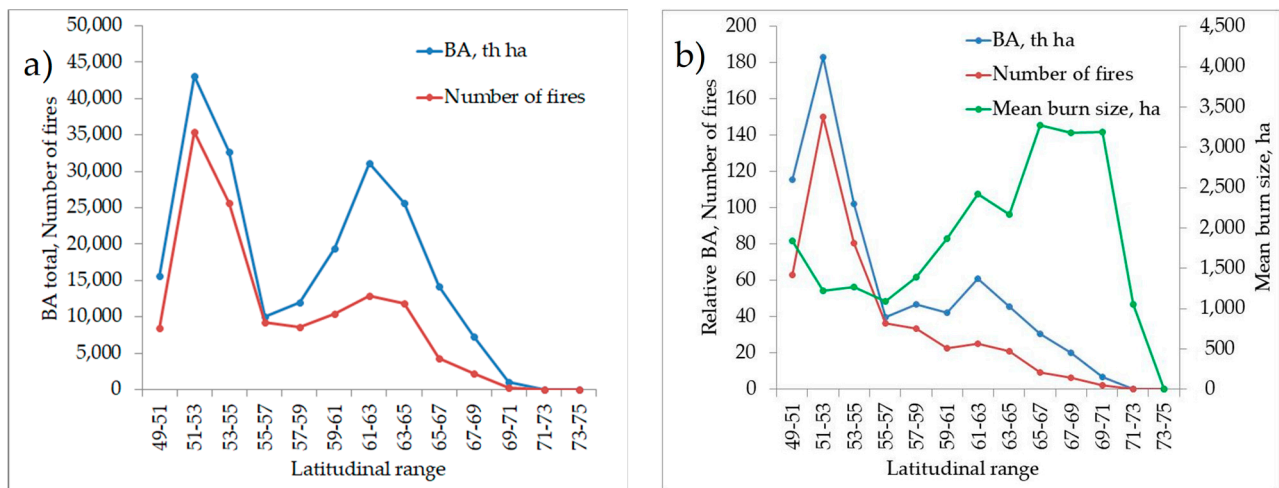


**Figure 4.** (a) Total burned area and number of fires reach their maximum values within the southern and northern parts of the larch range. (b) Relative burned area and number of fires. Values are normalized by the area of the larch forests within each latitudinal range. Study period is 1996–2022.

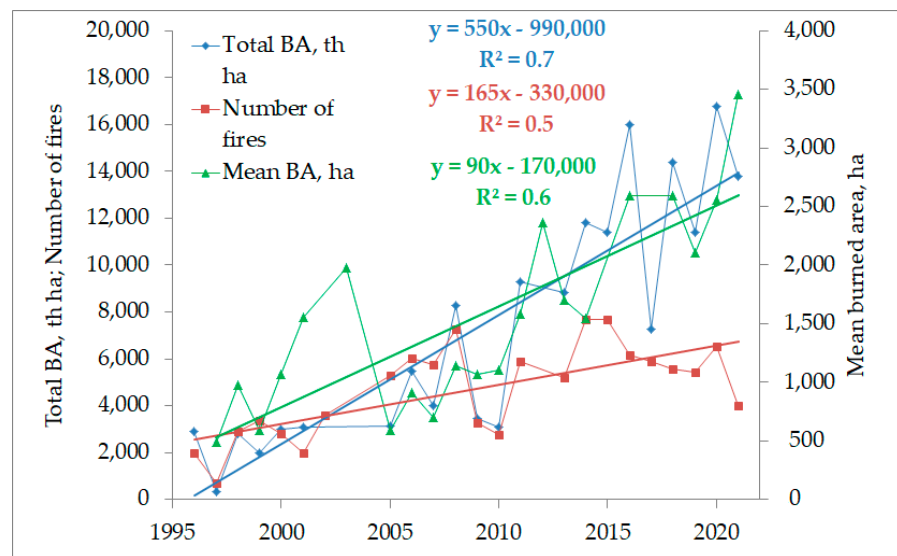
**Table 1.** Dependence of the annual burned area and the number of fires on the environmental variables.

| Study Area *   | Environmental Variables | Burned Area             |         | Fire Frequency          |          |
|----------------|-------------------------|-------------------------|---------|-------------------------|----------|
|                |                         | Adjusted R <sup>2</sup> | p-Value | Adjusted R <sup>2</sup> | p-Value  |
| Larch range ** | Air temperature         | 0.36                    | 0.0016  | 0.22                    | 0.026    |
|                | Precipitation           | 0.32                    | 0.041   | 0.21                    | 0.038    |
|                | Soil moisture           | 0.55                    | 0.0003  | 0.21                    | 0.047    |
|                | SPEI                    | 0.26                    | 0.012   | 0.17                    | 0.058    |
|                | TW                      | 0.28                    | 0.034   | 0.22                    | 0.065    |
| North **       | Air temperature         | 0.36                    | 0.0019  | 0.25                    | 0.047    |
|                | Precipitation           | 0.38                    | 0.02    | 0.46                    | 0.041    |
|                | Soil moisture           | 0.62                    | 0.0008  | 0.36                    | 0.015    |
|                | SPEI                    | 0.56                    | 0.0008  | 0.29                    | 0.037    |
|                | TW                      | –                       | –       | –                       | –        |
| South1 ***     | Air temperature         | 0.48                    | 0.0019  | 0.63                    | 0.0001   |
|                | Precipitation           | 0.31                    | 0.005   | 0.38                    | 0.0001   |
|                | Soil moisture           | 0.49                    | 0.0001  | 0.67                    | 0.000001 |
|                | SPEI                    | 0.23                    | 0.017   | 0.36                    | 0.002    |
|                | TW                      | 0.24                    | 0.06    | 0.31                    | 0.03     |
| South2 ***     | Air temperature         | 0.12                    | 0.087   | 0.13                    | 0.075    |
|                | Precipitation           | 0.14                    | 0.089   | 0.20                    | 0.036    |
|                | Soil moisture           | 0.48                    | 0.0001  | 0.46                    | 0.0002   |
|                | SPEI                    | 0.38                    | 0.0011  | 0.42                    | 0.0005   |
|                | TW                      | 0.32                    | 0.022   | 0.28                    | 0.035    |

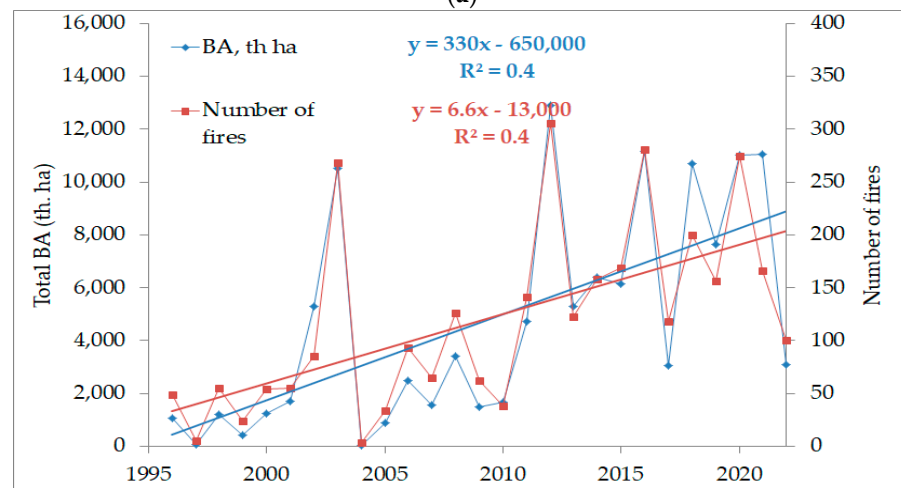
\* Study areas: Larch range on Figure 1; North—area 1 in Figure 1; South1 and South2—areas 2 and 3 in Figure 1, respectively. \*\* JJA period is for the northern study site. \*\*\* MJJAS period is for the southern study sites.

### 4.3. Wildfire Temporal Dynamics

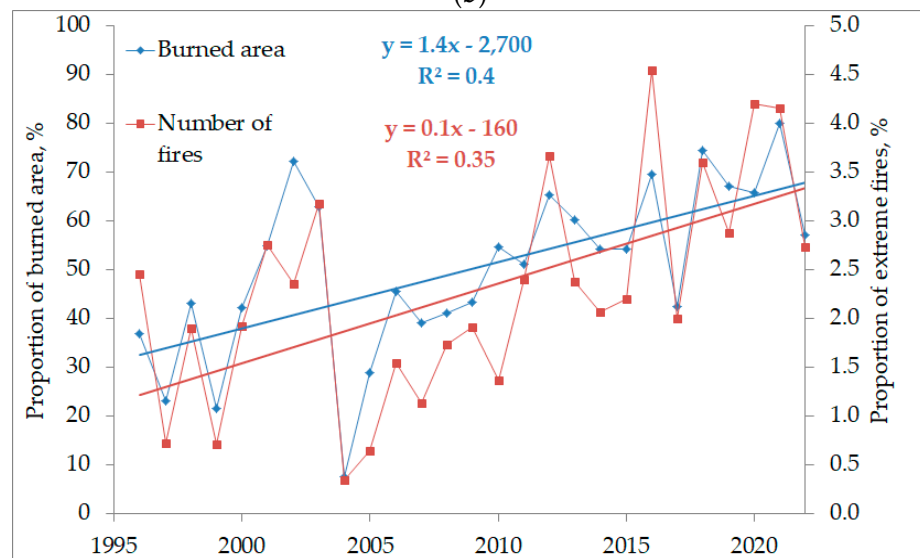
Since the late 1990s, the total burned area and mean burned area have been strongly increasing within the larch range. In the second decade (2012–2022 vs. 2001–2011), the mean burned area increased by about 2.0 times ( $p < 0.05$ ). The number of fires was also increasing in this period, albeit less strongly (Figure 5a). At the same time, the number of extreme fire events which caused a burned area of >10,000 ha also strongly increased (Figure 5b). The number of extreme fires and the burned area increased by factors of 2.7 and 3.6, respectively, in the second decade (2012–2022 vs. 2001–2011;  $p < 0.01$ ). The maximum registered burned area reached ~900,000 ha. The proportions of extreme fire events and the relevant burned area show increasing trends. Although the maximum proportion of extreme fire events was less than 5%, they were responsible for more than 80% of the annual burned area (Figure 5c).



(a)



(b)



(c)

**Figure 5.** (a) Total burned area, mean burned area, and the number of fires are increasing within the larch range. (b) Number of extreme fire events (fires with area burned >10,000 ha) and their area are increasing. (c) Proportion (in percent) of extreme fires and the corresponding burned area are increasing. Trends (without outliers in 2003 and 2022) are significant at  $p < 0.01$ .

#### 4.4. Wildfire Intensity

The majority of fires in the larch-dominant communities are considered to be low-intensity fires [42]. However, high-intensity fires occurred on the southern and especially on northern boundaries of the larch range (Figure 6).

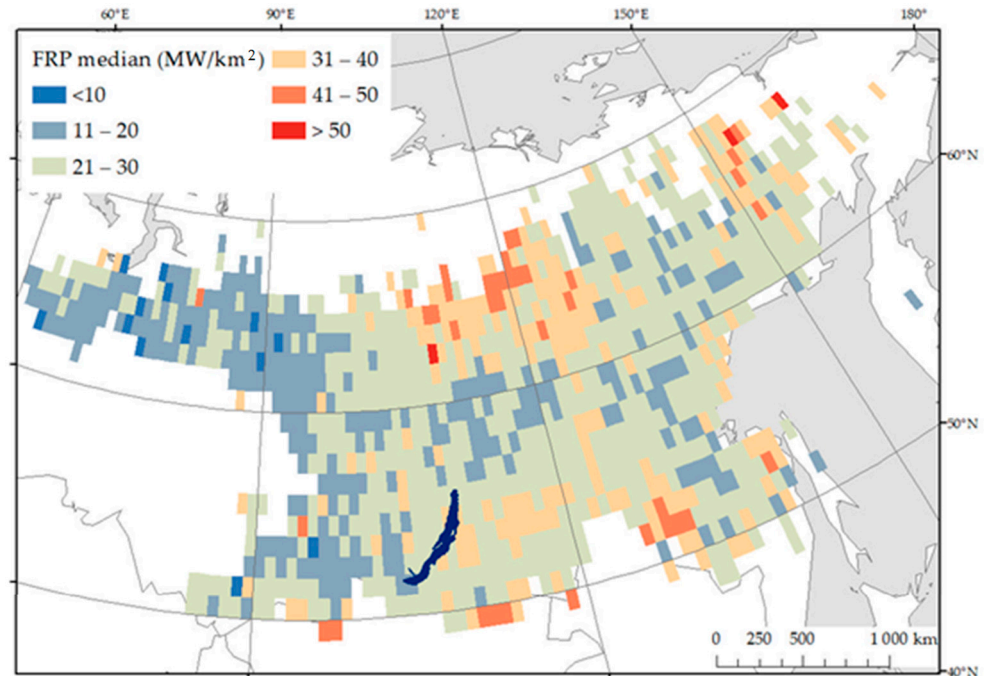


**Figure 6.** Spatial distribution of median fire radiative power (FRP;  $1 \times 1^\circ$  regular grid). High-intensity fires were located mostly in the northern part of the larch range and, to a lesser extent, in the southern one.

The proportion of high-intensity fires is 26% within the  $50\text{--}60^\circ\text{N}$  range and 29% within the  $60\text{--}70^\circ\text{N}$  range. The median FRP value for the  $60\text{--}70^\circ\text{N}$  range is 10% higher than that for the  $50\text{--}60^\circ\text{N}$  range (Figure 7a). Throughout the 21st century, fire intensity has been increasing (Figure 7b).

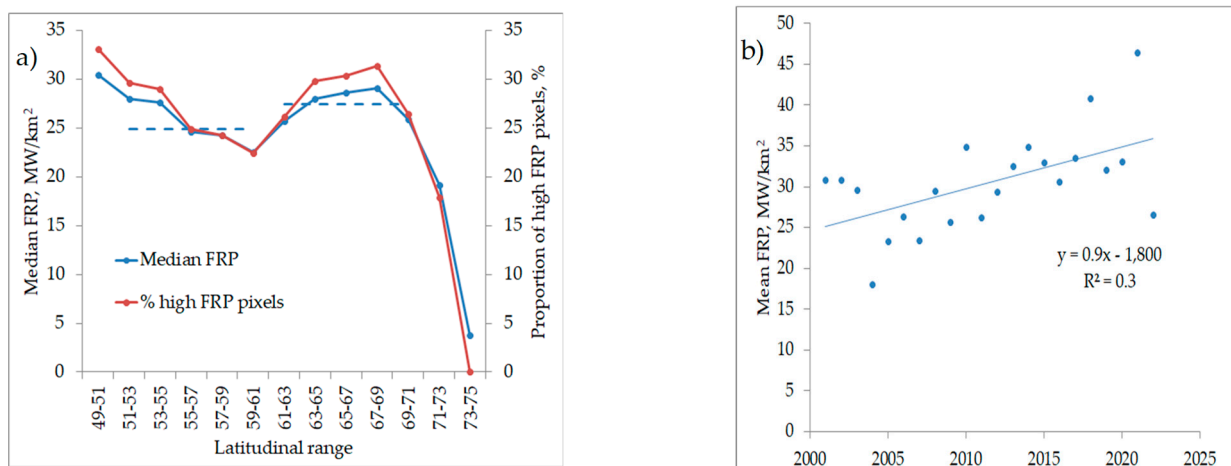


**Figure 7.** (a) Median values of fire radiative power (FRP) along the latitudinal gradient. The proportion of high-intensity fire pixels (FRP  $\geq 50$  MW) within each latitudinal range is shown in red. Dashed lines indicate median FRP values for the  $50\text{--}60^\circ\text{N}$  and  $60\text{--}70^\circ\text{N}$  latitude ranges. FRP is significantly higher in the  $60\text{--}70^\circ$  range ( $p < 0.01$ ). (b) The severity of fires is increasing ( $p < 0.05$ ). As a threshold for high-intensity fires, we used value of FRP  $> 50$  MW/km<sup>2</sup>, where FRP is fire radiative power [43,44].

#### 4.5. Wildfire Dependence on the Climate Variables

The dependence of the number of fires and the burned area on the climate variables is presented in Figure 8 (for the total larch range) and in Figure S2 and Table 1 for the northern and southern study areas. In all cases, increases in air temperature lead to exponential increases in fire rate (Figure 8a), whereas moisture parameters (precipitation, soil moisture, terrain water content, and the SPEI drought index) increases (i.e., air drought decrease) lead to decreases in both the number of fires and the area burned (Figure 8b–e). A notable fact is that for the northern study area, the strongest correlation between fire variables and soil moisture is observed for the 0–7 cm depth layer; whereas for the southern areas, the strongest correlations are observed for the 7–28 and 28–100 cm soil depth layers. This effect is due to the location of available water for vegetation at the deeper soil horizons in comparison with the northern site; this will have influenced “fuel readiness” (i.e., fuel dryness) for fire ignitions.

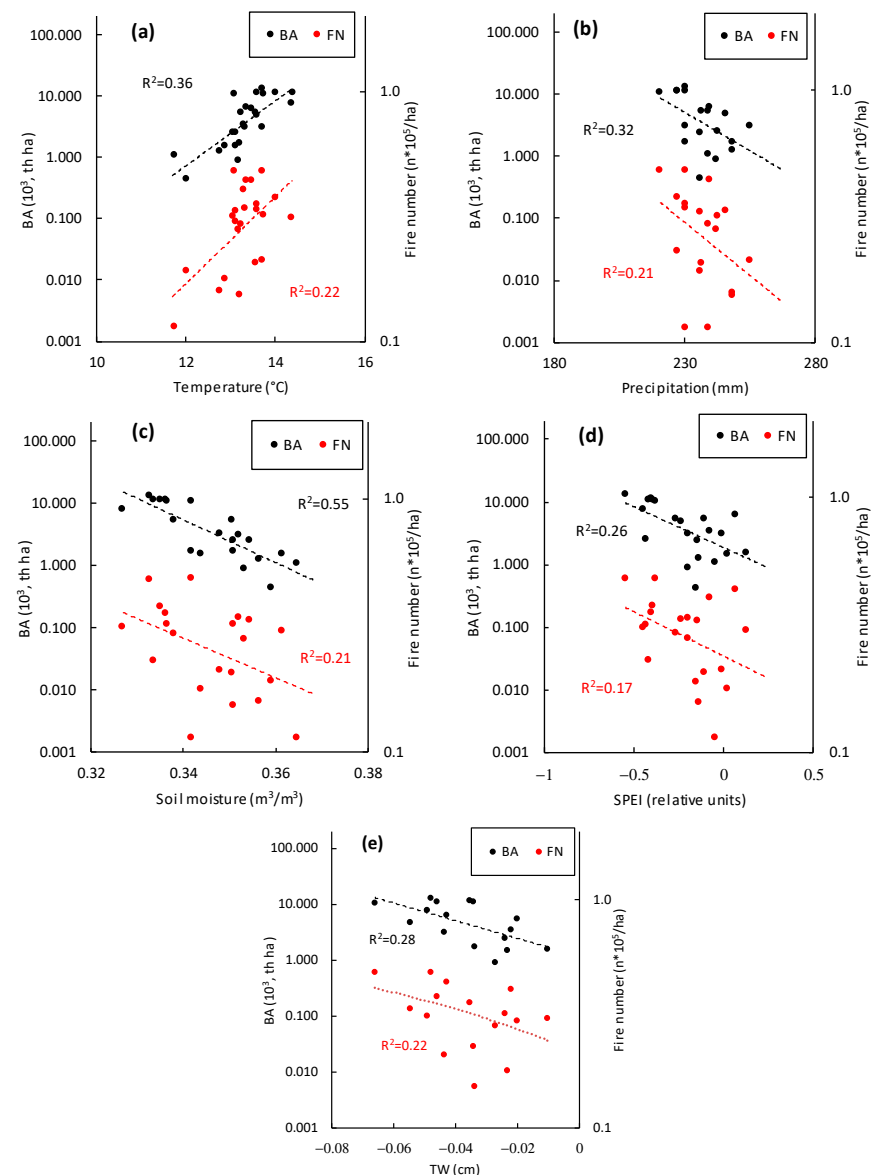


**Figure 8.** Dependence of extreme burned area ( $BA > 10,000$  ha) and the number of fires on environmental variables within the larch range in the permafrost zone (Figure 1). Both the burned area and the number of fires increase with the air temperature increase (a) and decrease with the precipitation (b), soil moisture (c), SPEI drought index (d), and terrestrial water content (e) increase. Soil moisture is considered within the upper (0–7 cm) soil level. Note that an SPEI decrease indicates air a drought decrease by definition. The considered fire season is JJA. Studied period is 2002–2022.

#### 4.6. Wildfire Influence on the Larch Trees' Growth

Larch species, especially *L. sibirica*, can survive multiple fires. The unique *L. sibirica* sample (presented in Figure 9a) experienced 13 fire events (in 1593, 1606, 1615, 1635, 1649, 1667, 1720, 1754, 1808, 1843, 1909, 1921, and 1966) (Figure 9a). After a fire, the growth index of surviving trees was increasing (Figure 9b). This post-fire growth increase occurred with a one-year lag (Figure 9c). Over time, larch growth decreases until the next fire (Figure 9b).

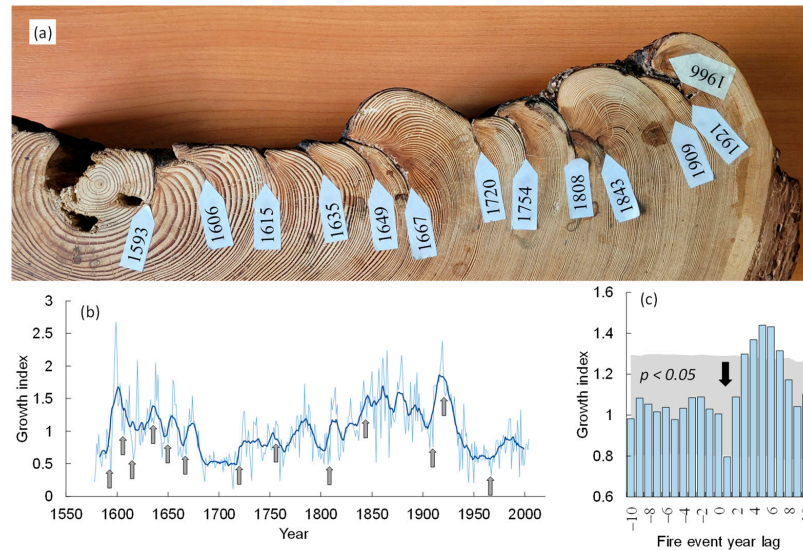


**Figure 9.** A specimen of larch (*L. sibirica*) trunk with multiple dated fire scars (a) and the corresponding dynamics of growth index (b). Fire events are shown by arrows; a solid line shows an 11 y moving average. Fire’s influence stimulated larch growth. (c) Post-fire growth increase occurred with a one-year lag (indicated by arrow). Date of fire is indicated by zero (“0”). Sample was taken at 61°36' N, 93°00' E.

Although air temperature is a primary determinant of larch growth in the permafrost zone, fire-induced larch growth was observed even in the periods when air temperature strongly decreased. Whereas air temperature was decreasing in the Little Ice Age, the larch experienced a strong post-fire growth increase (Figure 10). This post-fire larch growth was promoted by decreased species competition, improved radiation regime, an increased supply of nutrients, and increased root habitat zone due to permafrost melt [9].

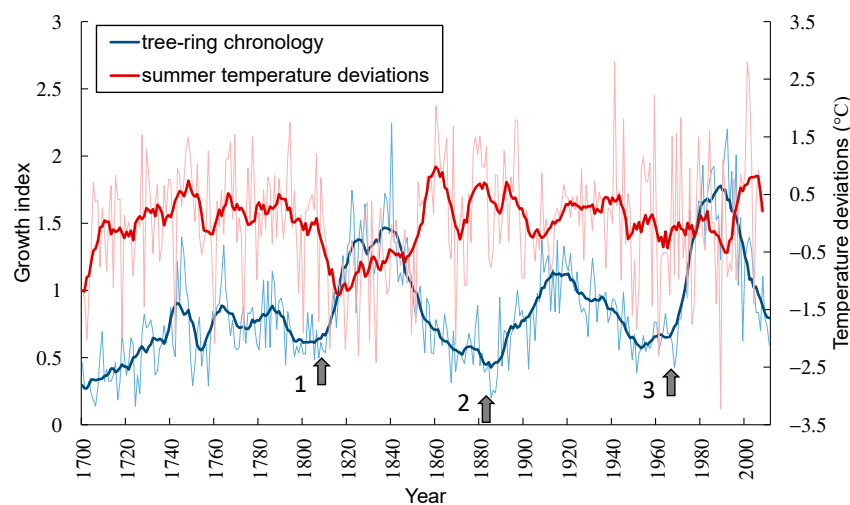


**Figure 10.** Post-fire growth index of larch (*Larix gmelinii*) trees vs. summer temperature deviations. Arrows indicate fire events; solid lines denote an 11 y moving average. Post-fire growth increase was observed even in the case of air temperature decrease (fire number 1). Samples (N = 20) were taken at 65°20' N/100°37' E (study area #1 in Figure 1).

#### 4.7. Post-Fire Regeneration within Burns

We analyzed post-fire regeneration on burns located within the northern (continuous permafrost) and southern (discontinuous and patched permafrost) areas of the larch (*L. gmelinii*, *L. sibirica*) range (study areas #1–3 in Figure 1).

##### (a) Post-fire regeneration in the continuous permafrost zone (study area #1)

Forests within study area #1 are formed of *Larix gmelinii*. In this area, larch regenerated successfully within burns. The seedling population within burns was composed mostly of *L. gmelinii* with an admixture of birch (*Betula* sp.) (Table 2). Siberian pine (*Pinus sibirica*) species occasionally populated burns which are located southward of the Arctic Circle. The amount of regeneration was dependent on the burn severity. Thus, if on-ground vegetation moss and lichen was mostly burned out, the number of larch seedlings may exceed 500,000 per ha (Figure 11d). Otherwise, the seedling population is considerably lower (3000 or less). Under the mother canopy, the number of seedlings is also considerably lower (ca. 600 or less specimen per ha (Figure 11a–c; Table 2)). Shrubs within burns are represented mostly by alder (*Duschekia fruticosa*), birch (*Betula* spp.), and willow species (*Salix* spp.). The population of small shrubs included *Vaccinium* sp., *Empetrum* sp., *Lydum* sp., and some other species.

**Table 2.** Seedling species composition and number per ha within larch-dominant forest and within burns at the study area #1 (Figure 1). The number of test sites was N = 25.

| Soil Type             | Forest and Burns      | Seedling Species Composition | Seedling Number (Thous. per ha)             |
|-----------------------|-----------------------|------------------------------|---|
| Permafrost gley soils | Larch-dominant forest | 10 L *                       | 0.33 ± 0.06 ***<br>(number of sites N = 13) |
|                       | Burns                 | 10 L + ** B                  | 40–500<br>(number of sites N = 12)          |

\* species composition at decimal scale; \*\* less than 5% of the total number; \*\*\* mean error ( $m_x$ ). Abbreviations: L—larch; B—birch.



**Figure 11.** (a) Northern *L. gmelinii* forest with rare fires (FRI, fire return interval, is about 300 years). Regeneration is negligible. Most trees are old (A = 300. . .500+ years). (b,c) Northern *L. gmelinii* forest with FRI of 70–150 years. Regeneration number is 200–1000 per ha. Larch (in front) survived several fires. (d) Fresh burn (A = ca.15 years) with abundant (>500,000 per ha) larch regeneration.

(b) Post-fire regeneration at the south of the larch range (study area #2)

The study area is located within the mid-mountain belt (1000–1600 m a.s.l.). Forests are represented by larch-dominant stands with an admixture of Siberian pine and spruce (*Picea obovata*). Observations were conducted within burns caused by surface fires (test sites number N = 32). Meanwhile, one observation was conducted within the burn that was caused by the crown fire. Generally crown fires are rare in the larch forests.

Under the canopy of a mature larch-dominant forest, seedling composition was represented mostly by non-larch species, and the regeneration amount was low (Table 3). After fire, the major pioneer grass species within burns are fireweed (*Epilobium angustifolium*) (“a fireweed burn”) and woodreed (*Calamagrostis* sp.) (“woodreed burn”). The regeneration rate is significantly dependent on the type of burn. Thus, on the “fireweed” burn, the regeneration amount is strongly (by a factor of 15) increased and represented mostly by larch seedlings (ca. 90%). However, within the “woodreed type” burn, i.e., the area with a dense grass ground cover, the regeneration amount is negligible (Table 3).

**Table 3.** Seedlings species composition and number per ha within forest and within burns at the study area South1. Test site number was N = 32.

| Soil Type   | Type of Forest and Burn | Seedling Species Composition  | Seedlings Number (Thous. per ha) |
|-------------|-------------------------|-------------------------------|----------------------------------|
| Loamy soils | Larch sedge-type forest | P2S2L *                       | 0.13                             |
|             | Fireweed burn           | 9L1SP + S and B               | 5.2 ± 0.31                       |
|             | Woodreed burn           | Seedling number is negligible |                                  |

\* species composition at decimal scale. Abbreviations: L—larch; B—birch; S—Scots pine; SP—Siberian pine.

(c) Study area #3

Within study area #3, larch-dominant stands are observed mostly on the mid and upper shadow slopes, as well as on the depressions with moist soils. Fires are of the surface type (“running” and “stable” surface fires), which causes about 40% of stands mortality in cases of long-lasting stable fires (Figure 12a).



**Figure 12.** (a) Larch (*L. gmelinii*) mortality after stable surface fire at the southern boundary of the larch range (the test area #3). (b) Post-fire woodreed meadow. Warming-driven recurrent fires turned sparse larch forests into steppe communities.

Similar to the southern area #2, the major pioneer grass species on burns are fireweed and woodreed. Summarized data on the number of seedlings and seedling species composition are presented in Table 4.

**Table 4.** Seedling species composition and the number of seedlings within the forest and burns at the study area South2 (Figure 1). The number of test sites was around 100.

| Soil Type   | Type of Forest and Burn | Seedling Species Composition | Seedlings Number (Thous Per ha) |
|-------------|-------------------------|------------------------------|---------------------------------|
| Loamy soils | Larch-dominant forest   | 6L3As1B                      | 6.2 ± 1.2                       |
|             | Fireweed burn           | 8B2L                         | 390 ± 87                        |
|             | Woodreed burn           | 6B3L1As                      | 17 ± 4.5                        |

Abbreviations: L—larch; B—birch; As—aspens.

After the fire, the number of seedlings on burns of the “fireweed” type strongly increased (more than fifty times). Meanwhile, the majority of the seedlings were represented by birch species. Within the woodreed burns, birch also dominated. However, the regeneration amount is comparatively poor, i.e., only exceeding regeneration under the mother canopy by about three times (Table 4). Under the current climate warming and drying and the increase in repeated fires, it is likely that a considerable part of the forested areas will transform into non-forest and steppe communities (Figure 12b).

Thus, we observed a contrasting response to fires in the core of the larch range (i.e., in continuous permafrost) and at the southern lowland boundary of the larch range. Within continuous permafrost, the burned areas regenerated with abundant larch seedlings; whereas in the transition to forest–steppe, the burned areas regenerated mostly with broadleaf species or, in extreme cases, turned into grass communities.

#### 4.8. Post-Fire GPP Dynamics

Within burned areas caused by surface fires, vegetation gross primary productivity (GPP) was restored within 3–5 and ca. 10 years (for the southern and northern sites, respectively). Crown fires caused the strongest impact on the GPP (about a two-times decrease) with a GPP recovery period of about 10–15 years (Figure 13). It is noteworthy that the post-fire growth increase has a one-year lag in the northern area; whereas in the southern sites, this lag may not be observed (Figure 13).

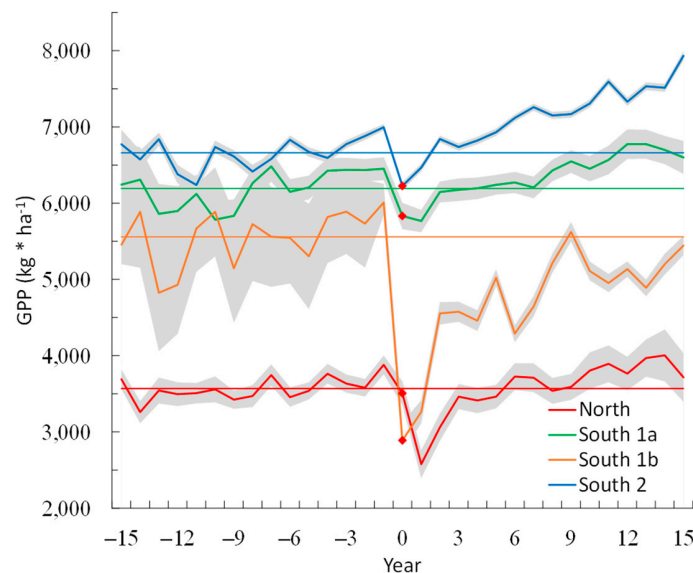


**Figure 13.** Post-fire GPP recovery patterns for the study areas North (202 burns), South 1a (336 burns), South 1b, and South 2 (2022 burns) (Figure 1). All burns, with the exception of South 1b, were caused by surface fires, whereas South 1b was caused by a crown fire (center point coordinates are 50° 37' N 95° 15' E). The crown fire occurred in the year 2002. GPP dispersion before that period was approximated via data collected on 101 test sites around that burn. The year of wildfire is indicated by zero (0) and marked by a red dot. Horizontal lines are mean GPP values for the pre-fire period. Shaded areas indicate a 95% confidence interval. Note that the post-fire growth increase has a one-year lag at the northern area and may not have a lag on the southern ones.

## 5. Discussion

### 5.1. Wildfire Dynamics in the Larch-Dominant Forests

Throughout the larch range, the annual area burned, number of fires, and fire severity are increasing in the permafrost zone. Note that not only total burned area but also a number of large (>200 ha) and extremely large (>10,000 ha) burns as well, as the mean burned area, are increasing (Figure 5). Moreover, the northern boundary of fire occurrence is migrating and has already reached the Arctic Ocean shore in eastern Siberia [13].

Geographically, the burned area is increasing in a northward direction, reaching its maximum within the 60°–70° N latitudes while the fire frequency is decreasing. This is followed by a sharp decrease in fire rate at higher latitudes due to lower insolation which results in insufficient fuel dryness (Figure 7). The larger burned area in the northern larch range is explained via higher fuel load and fuel warming-driven receptiveness to ignitions; whereas at lower latitudes, fuels are fragmented by clear-cuts. Together with this, wildfires at high latitudes are mostly not suppressed.

It is considered that the majority of fires in larch forests are of low intensity [42]. However, high-intensity wildfires occurred both in the southern and especially in the northern (60°–70° N) parts of the larch range (Figure 6), where the proportion of high-intensity fires exceeds 20%. During recent decades, fire intensity has been increasing due to the climate drying together with an increase in lightning-ignited fires (Figure 7b) [13].

The fire rate, including extreme fires, is exponentially correlated with the air temperature and moisture parameters (soil moisture, terrestrial water content, and SPEI drought index; Figures 8 and S2–S4). Meanwhile, fuel moisture is the primary determinant of wildfire occurrence. Air temperature and precipitation influenced the fire rate indirectly through fuel flammability. Note that in the north, the burned area and number of fires are better correlated with the soil moisture within the upper (0–7 cm) layer; whereas in the south, correlations are stronger with the moisture at deeper (7–28, 28–100 cm) layers. Thus, in a dryer southern climate, on-ground cover moisture (i.e., fuel receptiveness to ignitions) is dependent on the water content in the deeper soil horizons. Meanwhile, soil moisture decreases and air drought increases in the larch range (Figure 2b–e) are potentially increasing the likelihood that a given fire ignition will result in a wildfire.

At high latitudes, warming-driven lightning frequency is also an important determinant of the burning rate [11]. An increase in lightning-caused wildfires was reported for forests in North America [10] and the Siberian Arctic [13]. Although global warming will lead to a decrease in the frequency of lightning, in the boreal region, lightning activity will increase [12]. Consequently, lightning has the potential to further increase the burning rate throughout the permafrost zone.

### 5.2. Wildfire and Larch Dominance in the Permafrost

Burned areas regularly include a mosaic of living tree clusters because of relief complexity which allows trees to survive stand-replacing fires. In addition, the larch itself is resistant to fires and can restore itself after consecutive fires (Figure 9a). That refugia serves as a seed source for larch regeneration. Moreover, already-ripe seeds in the mother canopy also supply the burns with seeds because the cones open in winter or spring. Wind and melt water spread the winged, light larch seeds into burned bare surfaces that are suitable for seeds rooting. Regeneration abundance is facilitated via soil enrichment with phosphorus, potassium, nitrogen, and other nutrients, as well as via improved soil aeration and drainage and a deeper active layer. Upper canopy elimination improves the light regime, which is important for the photophilic larch (Figure 11d).

Larch trees can survive multiple fires. With a one-year lag after a fire, surviving trees experience increased growth (Figure 9c). Over time, larch growth on permafrost decreases due to the seasonal melting layer decrease caused by the growth of the moss and lichen matrix, a heat insulator, with consequent active layer shrinking. The growth of that matrix also decreases seedling establishment because the matrix traps larch seeds and prevents seed rooting. The decrease in nutrients supply also leads to growth decrease

(Figure 9b). Larch trees fall into stagnation, awaiting the next fire that will be facilitated via fuel accumulation, dry weather, and increased warming-driven lightning ignitions. Thus, periodic fires determine the larch dominance within the permafrost zone. Fires formed the larch forest as a mosaic of semi, even-age stands at different phases of post-fire succession.

We observed a contrasting response to fires in the continuous permafrost and at the southern lowland boundary of the larch range. In the first case, larch seedlings are typically vigorous and abundant (up to >500,000 per ha), while under the mother canopy, the regeneration number is two-three orders lower (Table 2). Alongside larch, birch (*Betula* spp.) and alder (*Duschekia fruticosa*) also participate in regeneration, although more often within wind-sheltered relief features. Earlier, it was shown that burns also served as “starting places” for Siberian pine (*Pinus sibirica*) trees in climate-driven northward migration as well as for the other relatively less cold-tolerant species, e.g., *Abies sibirica*, *Picea obovata* [43].

Within the southern part of the larch range, larch regeneration is less successful; the number of seedlings is two orders lower than on the northern site (Tables 3 and 4). Even in the case of abundant regeneration, the majority of seedlings (up to 80%) are represented by hardwood species (Table 4). Amplified burning in the south may lead to the transformation of larch forests into grass and shrub communities within discontinuous and patched permafrost zones (Figure 12b). We suggested that permafrost melting potentially decreases larch-dominance by increasing the proportion of relatively southern species (e.g., birch and aspen) in the forests structure. Permafrost melting also leads to the formation of ponds and bogs as well as grass communities [44], although the geography and dynamics of these events needs more study. At the same time, in the southern highlands, larch is migrating into alpine tundra and increasing growth [25].

The other potential consequence of permafrost melting is substitution of *L. gmelinii* by *L. sibirica* due to differences in fire adaptation strategies. Thus, *L. sibirica* is protected against surface fires by thick bark that provides thermal isolation to living tissues while the roots are located in rather deep soil; whereas *L. gmelinii* has thinner bark since it grows mostly within permafrost where the majority of mortality is caused via thermal damage to roots that are located within the thin active layer (up to 30 cm or less).

Within burns in the south, vegetation GPP quickly restores and even exceeds pre-fire values within 3–5 years. Meanwhile, crown fires have a strong impact on GPP, with follow-on recovery taking about 10–15 years (Figure 13). A strong decrease in larch forest productivity after severe fires was also reported for the northeastern China [45]. Notably, crown fires are rare events in the larch forest; they were never reported in the northern areas where larch formed low closure stands due to “cold permafrost soils” and a narrow active layer. Post-fire quick restore of GPP indicated that in spite of fires, larch forests continue to serve as a carbon stock. These results support recent data on the increase in above-ground biomass in the Russian boreal forests [27].

In addition, fires promote biodiversity support. Typically, on-ground vegetation under the larch canopy is presented by a few grass and bush species [24]. Birch, alder, willow, and—within the southern range—aspens are the pioneer settlers on burns. A number of grass species (fireweed, woodreed, graminoids, and others) and fruit-bearing shrubs that are important to animals (currants, viburnum, raspberry, blueberries, cowberry, honeysuckle) populate burns, especially in the middle and southern parts of the larch range [9]. Increased vegetation biodiversity is attracting animals such as moose, elk, and bear. Sables are coming to burns due to the increased populations of hares and mouse-like rodents.

In summary, while recurrent wildfires occurred within larch-dominant communities throughout Holocene, permanent larch forest growth and its vigor indicated that periodic natural fires are a prerequisite condition for larch growth and dominance within the permafrost zone; wildfires reset the larch forest’s vigor and contribute to the renewal of larch ecosystems. Consequently, there is no necessity for complete fire suppression within permafrost.

### 5.3. Firefighting in the Larch-Dominant Forests

Due to the increased fire rate, modification to the fire suppression strategy within the larch-dominant zone is required. It is known that the complete suppression of fires leads to fuel accumulation that can result in catastrophic fires. At the landscape level, natural fires are a necessary tool in the fire suppression strategy in permafrost because other methods (e.g., prescribed fires, removal of fuel) are not applicable across extensive northern forest ecosystems [18,19]. Periodic fires reduce the likelihood of catastrophic fires and contribute to the conservation and restoration of larch-dominated communities.

In conditions of increased burning, the impact of fires will increase, whereas the possibility of fire suppression will decrease. Therefore, researchers have suggested a paradigm change by which to allow more wildfires to burn across extensive forest landscapes [9,17]. Instead of complete fire suppression, we suggest monitoring wildfires that are allowed to burn under acceptable conditions, with fire suppression only in cases when there is potential danger to people, protected areas, and at-risk assets. Such an approach is already being adopted in areas with constraints on fire suppression. In fact, in the northern territories of Siberia and Canada, wildfires are not suppressed unless they threaten humans and at-risk assets [17].

Furthermore, the ecological importance of fire is increasingly being recognized; for example, early policy in Alaska focused on the suppression and prevention of as many fires as possible despite limited resources [18,19,46]. However, given the infeasibility of suppressing all wildfires and the growing understanding of the ecological role of fire, the fire strategy shifted to a wildfire management approach wherein fire is allowed on the landscape (where and when appropriate), thereby allowing for natural fire-supporting dynamics and ecological processes [9,18].

## 6. Conclusions

Throughout the larch range, warming amplified the fire frequency and area burned. Warming leads to increases in fire severity and extreme fire events (with burned area > 10,000 ha). Although the proportion of extreme fires was less than 5%, such fires are responsible for more than 80% of the burned area. The fire rate exponentially increases with decreases in soil moisture and increases in air temperature and air drought. Geographically, the burned area is increasing northward while fire frequency is decreasing.

Wildfire impact on regeneration contrasts within continuous permafrost and within the southern lowlands of the larch range. In the north, fire promotes successful larch regeneration (up to 500,000+ seedlings per ha); whereas in the south, post-fire regeneration is composed mostly of broadleaf species or the area is turned into grass communities. We suggested that the thawing of continuous permafrost would lead to shrinking larch dominance in the south. The other potential consequence of permafrost melting is the substitution of *L. gmelinii* by *L. sibirica* due to differences in the fire resilience strategies of these species.

Notably, a quick (3–15 years) vegetation GPP restores the pre-fire levels, which may indicate that in spite of fires, larch forests continue to serve as a carbon stock.

In summary, periodic fires are a prerequisite of successful larch regeneration and resilience within continuous permafrost. Therefore, it is not necessary to suppress all fires within the zone of larch dominance. Instead, we must focus fire suppression on areas of high natural, social, and economic importance, while permitting the majority fires burning in vast larch-dominant permafrost landscapes.

Some future prospects of this study include (1) investigations into pyrogenic successions within the transition between the continuous permafrost and non-permafrost areas (e.g., “southern” species invasion); (2) studies of the potential warming-driven larch range shrink; and (3) studies of the substitution of *L. gmelinii* by *L. sibirica* within the southern part of *L. gmelinii* range.

**Supplementary Materials:** The following supporting information can be downloaded at: <https://www.mdpi.com/article/10.3390/fire6080301/s1>. Figure S1. Tree species composition map within permafrost zone. Based on the VEGA-PRO map (<http://pro-vega.ru/eng/> (accessed 14 July 2023)). Figure S2. Study area North (Figure 1). Dependence of the annual wildfire North (BA > 200 ha) occurrence on the (a) air temperature, (b) precipitation, (c) soil moisture (with 0–7 cm soil depth), (d) SPEI drought index and (e) terrestrial water content. Study period 1996–2022 with exception for TW (2002–2022). Climate variables considered for JJA period. Figure S3. Study area South1 (Figure 1). Dependence of the annual burned area and fires number on the (a) air temperature, (b) precipitation, (c) soil moisture (with 7–28 cm soil depth), (d) SPEI drought index and (e) terrestrial water content. Study period 1996–2022 with exception for TW (2002–2022). Climate variables considered for JJA period. Large fires (i.e., BA > 200 ha with exception for (a): BA > 1000 ha) were considered. Figure S4. Study area South2 (Figure 1). Dependence of the annual burned area (large fires, BA > 200 ha) and fires number on the (a) air temperature, (b) precipitation, (c) soil moisture (28–100 cm soil depth), (d) SPEI drought index and (e) terrestrial water content. Study period 1996–2022 with exception for TW (2002–2022). Climate variables considered for MJJAS period.

**Author Contributions:** Conceptualization, V.I.K.; methodology, V.I.K. and E.G.S.; validation, V.I.K. and A.S.G.; formal analysis, E.G.S., L.V.B. and A.S.G.; investigation, V.I.K.; E.G.S. and L.V.B.; resources, E.G.S., M.L.D., A.S.G. and I.A.P.; data curation, E.G.S., M.L.D., A.S.G. and I.A.P.; writing—original draft preparation, V.I.K.; writing—review and editing, V.I.K.; visualization, E.G.S., M.L.D., A.S.G. and I.A.P.; supervision, V.I.K.; project administration, V.I.K.; funding acquisition, V.I.K. All authors have read and agreed to the published version of the manuscript.

**Funding:** This research was funded by the Tomsk State University Development Program («Priority2030»).

**Institutional Review Board Statement:** Not applicable.

**Informed Consent Statement:** Not applicable.

**Data Availability Statement:** Publicly available datasets were analyzed in this study. Thermal anomaly products were downloaded using the LAADS (Level-1 Atmosphere Archive and Distribution System) service (<https://ladsweb.modaps.eosdis.nasa.gov/>) (accessed on 11 May 2023); the ERA5-Land dataset, available online: <https://cds.climate.copernicus.eu/cdsapp#!/dataset/reanalysis-era5-land-monthly-means?tab=overview> (accessed on 9 June 2023); SPEI (Standardized Precipitation Evaporation Index) available online: <https://spei.csic.es/map/maps.html> (accessed on 9 June 2023); GFZ GRACE/GRACE-FO EWTA data, available online: <https://podaac-opendap.jpl.nasa.gov/opendap/hyrax/allData/tellus/L3> (accessed on 9 June 2023); and the MODIS product, MOD17A3HGF, available online: <https://search.earthdata.nasa.gov/search?q=MOD17A3HGF> (accessed on 25 May 2023).

**Conflicts of Interest:** The authors declare no conflict of interest. The funders had no role in the design of the study; in the collection, analyses, or interpretation of data; in the writing of the manuscript; or in the decision to publish the results.

## References

- Bowman, D.; Balch, J.K.; Artaxo, P.; Bond, W.J.; Carlson, J.M.; Cochrane, M.A.; D'antonio, C.M.; Defries, R.S.; Doyle, J.C.; Harrison, S.P.; et al. Fire in the Earth system. *Science* **2009**, *324*, 481–484. [[CrossRef](#)]
- Krawchuk, M.A.; Moritz, M.A.; Parisien, M.-A.; Van Dorn, J.; Hayhoe, K. Global pyrogeography: The current and future distribution of wildfire. *PLoS ONE* **2009**, *4*, e5102. [[CrossRef](#)] [[PubMed](#)]
- Archibald, S.; Lehmann, C.E.R.; Belcher, C.M.; Bond, W.J.; Bradstock, R.A.; Daniou, A.L.; Dexter, K.G.; Forrestel, E.J.; Greve, M.; He, T.; et al. Biological and geophysical feedbacks with fire in the Earth system. *Environ. Res. Lett.* **2018**, *13*, 033003. [[CrossRef](#)]
- McLauchlan, K.K.; Higuera, P.E.; Miesel, J.; Rogers, B.M.; Schweitzer, J.; Shuman, J.K.; Tepley, A.J.; Varner, J.M.; Veblen, T.T.; Adalsteinsson, S.A.; et al. Fire as a fundamental ecological process: Research advances and frontiers. *J. Ecology* **2020**, *108*, 2047–2069. [[CrossRef](#)]
- Chapin, F.S.; Trainor, S.F.; Huntington, O.; Lovcraft, A.L.; Zavaleta, E.; Natcher, D.C.; McGuire, A.D.; Nelson, J.L.; Ray, L.; Calef, M.; et al. Increasing wildfire in Alaska's boreal forest: Pathways to potential solutions of a wicked problem. *BioScience* **2008**, *58*, 531–540. [[CrossRef](#)]
- Flannigan, M.; Stocks, B.; Turetsky, M.; Wotton, M. Impacts of climate change on fire activity and fire management in the circumboreal forest. *Glob. Chang. Biol.* **2009**, *15*, 549–560. [[CrossRef](#)]
- Kukavskaya, E.A.; Buryak, L.V.; Shvetsov, E.G.; Conard, S.G.; Kalenskaya, O.P. The impact of increasing fire frequency on forest transformations in southern Siberia. *For. Ecol. Manag.* **2016**, *382*, 222–230. [[CrossRef](#)]

8. De Groot, W.J.; Flannigan, M.D.; Cantin, A.S. Climate change impacts on future boreal fire regimes. *For. Ecol. Manag.* **2013**, *294*, 35–44. [CrossRef]
9. Kharuk, V.I.; Ponomarev, E.I.; Ivanova, G.A.; Dvinskaya, M.L.; Coogan, S.C.P.; Flannigan, M.D. Wildfires in the Siberian taiga. *Ambio* **2021**, *50*, 1953–1974. [CrossRef]
10. Veraverbeke, S.; Rogers, B.; Goulden, M.; Jandt, R.; Miller, C.; Wiggins, E.; Randerson, J. Lightning as a major driver of recent large fire years in North American boreal forests. *Nat. Clim. Chang.* **2017**, *7*, 529–534. [CrossRef]
11. Hessilt, T.D.; van der Werf, G.; Abatzoglou, J.T.; Scholten, R.C.; Veraverbeke, S. Future increases in lightning-ignited boreal fires from conjunct increases in dry fuels and lightning. In Proceedings of the 23rd EGU General Assembly, Online, 19–30 April 2021; EGU21-2218. Available online: <https://meetingorganizer.copernicus.org/EGU21/EGU21-2218.html> (accessed on 14 June 2023).
12. Finney, D.L.; Doherty, R.M.; Wild, O.; Stevenson, D.S.; MacKenzie, J.A.; Blyth, A.M. A projected decrease in lightning under climate change. *Nat. Commun.* **2018**, *8*, 210–213. [CrossRef]
13. Kharuk, V.I.; Dvinskaya, M.L.; Im, S.T.; Golyukov, A.S.; Smith, K.T. Wildfires in the Siberian Arctic. *Fire* **2022**, *5*, 106. [CrossRef]
14. Flannigan, M.D. Fighting fire with science. *Nature* **2019**, *576*, 328. [CrossRef]
15. Moritz, M.; Batllori, E.; Bradstock, R.; Gill, A.M.; Handmer, J.; Hessburg, P.F.; Leonard, J.; McCaffrey, S.; Odion, D.C.; Tania Schoennagel, T.; et al. Learning to coexist with wildfire. *Nature* **2014**, *515*, 58–66. [CrossRef]
16. Coogan, S.C.P.; Robinne, F.-N.; Jain, P.; Flannigan, M.D. Scientists’ warning on wildfire—A Canadian perspective. *Can. J. For. Res.* **2019**, *49*, 58–66. [CrossRef]
17. Tymstra, C.; Stocks, B.; Cai, X.; Flannigan, M. Wildfire management in Canada: Review, challenges and opportunities. *Prog. Disaster Sci.* **2020**, *5*, 10004. [CrossRef]
18. Wotton, B.M.; Flannigan, M.D.; Marshall, G.A. Potential climate change impacts on fire intensity and key wildfire suppression thresholds in Canada. *Environ. Res. Lett.* **2017**, *12*, 095003. [CrossRef]
19. Melvin, A.M.; Murray, J.; Boehlert, B.; Martinich, J.A.; Rennels, L.; Rupp, T.S. Estimating wildfire response costs in Alaska’s changing climate. *Clim. Chang.* **2017**, *141*, 783–795. [CrossRef]
20. Sannikov, S.N. Forest fires as a factor in transformation of the structure, renewal and evolution of biogeocenoses. *Ecology* **1981**, *6*, 23–33. (In Russian)
21. Hopkins, T.; Larson, A.; Belote, T. Contrasting Effects of Wildfire and Ecological Restoration in Old-Growth Western Larch Forests. *For. Sci.* **2014**, *60*, 1005–1013. [CrossRef]
22. Moris, J.V.; Vacchiano, G.; Ascoli, D.; Motta, R. Alternative stable states in mountain forest ecosystems: The case of European larch (*Larix decidua*) forests in the western Alps. *J. Mt. Sci.* **2017**, *14*, 811–822. [CrossRef]
23. Kharuk, V.I.; Dvinskaya, M.L.; Petrov, I.A.; Im, S.T.; Ranson, K.J. Larch Forests of Middle Siberia: Long-Term Trends in Fire Return Intervals. *Environ. Res. Lett.* **2015**, *16*, 2389–2397. [CrossRef] [PubMed]
24. Kharuk, V.I.; Ranson, K.J.; Petrov, I.A.; Dvinskaya, M.L.; Im, S.T.; Golyukov, A.S. Larch (*Larix dahurica* Turcz) Growth Response to Climate Change in the Siberian Permafrost Zone. *Reg. Environ. Chang.* **2018**, *1*, 233–243. [CrossRef]
25. Kharuk, V.I.; Petrov, I.A.; Golyukov, A.S.; Dvinskaya, M.L.; Im, S.T.; Shushpanov, A.S. Larch growth across thermal and moisture gradients in the Siberian Mountains. *J. Mt. Sci.* **2023**, *20*, 101–114. [CrossRef]
26. Shuman, J.K.; Shugart, H.H.; O’Halloran, T.L. Sensitivity of Siberian larch forests to climate change. *Glob. Chang. Biol.* **2011**, *17*, 2370–2384. [CrossRef]
27. Xu, L.; Saatchi, S.S.; Yang, Y.; Yu, Y.; Pongratz, J.; Bloom, A.A.; Bowman, K.; Worden, J.; Liu, J.; Yin, Y.; et al. Changes in global terrestrial live biomass over the 21st century. *Sci. Adv.* **2021**, *7*, eabe9829. [CrossRef]
28. Brown, J.; Ferriars, O.J.; Heginbottom, J.A.; Melnikov, E.S. *Circum-Arctic Map of Permafrost and Ground Ice Conditions, Ver. 2*; Digital Media; National Snow and Ice Data Center: Boulder, CO, USA, 2002. Available online: <https://nsidc.org/data/ggd318> (accessed on 24 April 2023).
29. Bartalev, S.; Egorov, V.; Zharko, V.; Loupian, E.; Plotnikov, D.; Khvostikov, S.; Shabanov, N. *Land Cover Mapping over Russia using Earth Observation Data*; Russian Academy of Sciences, Space Research Institute: Moscow, Russia, 2016; p. 208.
30. Hersbach, H.; Rosnay, P.; Bell, B.; Schepers, D.; Simmons, A.; Soci, C.; Abdalla, S.; Alonso-Balmaseda, M.; Balsamo, G.; Bechtold, P.; et al. Operational Global Reanalysis: Progress, Future Directions and Synergies with NWP. ECMWF ERA Report Series. 2018. Available online: <https://www.ecmwf.int/en/elibrary/18765-operational-global-reanalysis-progress-future-directions-and-synergies-nwp> (accessed on 19 July 2021).
31. Vicente-Serrano, S.M.; Beguería, S.; López-Moreno, J.I. A multiscalar drought index sensitive to global warming. The standardized precipitation evapotranspiration index. *J. Clim.* **2010**, *23*, 1696–1718. [CrossRef]
32. Landerer, F.W.; Flechtner, F.M.; Save, H.; Webb, F.H.; Bandikova, T.; Bertiger, W.I.; Bettadpur, S.V.; Byun, S.H.; Dahle, C.; Dobslaw, H.; et al. Extending the global mass change data record: GRACE Follow-On instrument and science data performance. *Geophys. Res. Lett.* **2020**, *47*, e2020GL088306. [CrossRef]
33. Giglio, L.; Schroeder, W.; Hall, J.V.; Justice, C.O. *MODIS Collection 6 and Collection 6.1 Active Fire Product User’s Guide*; National Aeronautical and Space Administration—NASA: Washington, DC, USA, 2021; p. 64.
34. Forest Management Instruction. Available online: <https://docs.cntd.ru/document/351878696> (accessed on 14 June 2023). (In Russian)
35. Regulations for reforestation. Ministry of Natural Resources of Russia. Available online: <https://docs.cntd.ru/document/728111110> (accessed on 14 June 2023). (In Russian)

36. Rinn, F.; Tsap, V. *3.6 Reference Manual: Computer Program for Tree-Ring Analysis and Presentation*; Frank Rinn Distribution: Heidelberg, Germany, 1996.
37. Holmes, R.L. Computer-assisted quality control in tree-ring dating and measurement. *Tree-Ring Bull.* **1983**, *44*, 69–75.
38. Cook, E.R.; Holmes, R.L. User's Manual for Program ARSTAN. In *Tree-Ring Chronologies of Western North America: California, Eastern Oregon and Northern Great Basin*; Chronology Series 6; Holmes, R.L., Adams, R.K., Fritts, H.C., Eds.; Laboratory of Tree-Ring Research: Tucson, TX, USA, 1986; pp. 50–65.
39. Sutherland, E.K.; Brewer, P.W.; Falk, D.A.; Vel'asquez, M.E. *FHAES Fire History Analysis and Exploration System (for FHAES Version 2.0.2)*; Missoula Forestry Sciences Lab: Missoula, MT, USA, 2017.
40. Fritts, H.C. *Tree-Rings and Climate/London*; Acad. Press: San Francisco, CA, USA; New York, NY, USA, 1976; 576p.
41. Running, S.; Mu, Q.; Zhao, M. *MODIS/Terra Net Primary Production Gap-Filled Yearly L4 Global 500m SIN Grid V061*; NASA EOSDIS Land Processes DAAC: Washington, DC, USA, 2021. [[CrossRef](#)]
42. Wooster, M.J.; Zhang, Y.H. Boreal forest fires burn less intensely in Russia than in North America. *Geophys. Res. Lett.* **2004**, *31*, L20505. [[CrossRef](#)]
43. Kharuk, V.I.; Ranson, K.J.; Dvinskaya, M.L. Evidence of evergreen conifer invasion into larch dominated forests during recent decades in Central Siberia. *Eurasian J. For. Res.* **2007**, *10*, 163–171.
44. Berner, L.T.; Beck, P.S.A.; Loranty, M.M.; Alexander, H.D.; Mack, M.C.; Goetz, S.J. Cajander larch (*Larix cajanderi*) biomass distribution, fire regime and post-fire recovery in northeastern Siberia. *Biogeosciences* **2012**, *9*, 3943–3959. [[CrossRef](#)]
45. Cai, W.; Yang, J. High severity fire reduces early successional boreal larch forest aboveground productivity by shifting stand density in north-eastern China. *Int. J. Wild. Fire* **2016**, *25*, 861–875. [[CrossRef](#)]
46. Todd, S.K.; Jewkes, H.A. Wildland fire in Alaska: A history of organized fire suppression and management in the Last Frontier. In *University of Alaska Fairbanks, Agricultural and Forestry Experiment Station Bulletin No. 114*; University of Alaska Fairbanks: Fairbanks, AK, USA, 2006.

**Disclaimer/Publisher's Note:** The statements, opinions and data contained in all publications are solely those of the individual author(s) and contributor(s) and not of MDPI and/or the editor(s). MDPI and/or the editor(s) disclaim responsibility for any injury to people or property resulting from any ideas, methods, instructions or products referred to in the content.